Comparison of a 3-D CFD-DSMC Solution Methodology With a Wind Tunnel Experiment

Christopher E. Glass and Thomas J. Horvath
Langley Research Center, Hampton, Virginia

Since its founding, NASA has been dedicated to the advancement of aeronautics and space science. The NASA Scientific and Technical Information (STI) Program Office plays a key part in helping NASA maintain this important role.

The NASA STI Program Office is operated by Langley Research Center, the lead center for NASA's scientific and technical information. The NASA STI Program Office provides access to the NASA STI Database, the largest collection of aeronautical and space science STI in the world. The Program Office is also NASA's institutional mechanism for disseminating the results of its research and development activities. These results are published by NASA in the NASA STI Report Series, which includes the following report types:
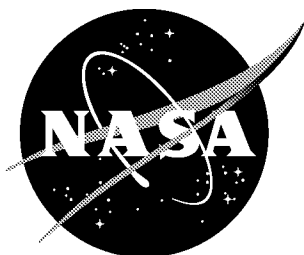
- TECHNICAL PUBLICATION. Reports of completed research or a major significant phase of research that present the results of NASA programs and include extensive data or theoretical analysis. Includes compilations of significant scientific and technical data and information deemed to be of continuing reference value. NASA counterpart of peer-reviewed formal professional papers, but having less stringent limitations on manuscript length and extent of graphic presentations.

- TECHNICAL MEMORANDUM. Scientific and technical findings that are preliminary or of specialized interest, e.g., quick release reports, working papers, and bibliographies that contain minimal annotation. Does not contain extensive analysis.

- CONTRACTOR REPORT. Scientific and technical findings by NASA-sponsored contractors and grantees.

- CONFERENCE PUBLICATION. Collected papers from scientific and technical conferences, symposia, seminars, or other meetings sponsored or co-sponsored by NASA.

- SPECIAL PUBLICATION. Scientific, technical, or historical information from NASA programs, projects, and missions, often concerned with subjects having substantial public interest.

- TECHNICAL TRANSLATION. English-language translations of foreign scientific and technical material pertinent to NASA's mission.

Specialized services that complement the STI Program Office's diverse offerings include creating custom thesauri, building customized databases, organizing and publishing research results ... even providing videos.

For more information about the NASA STI Program Office, see the following:

- Access the NASA STI Program Home Page at *http://www.sti.nasa.gov*

- E-mail your question via the Internet to help@sti.nasa.gov

- Fax your question to the NASA STI Help Desk at (301) 621-0134

- Phone the NASA STI Help Desk at (301) 621-0390

- Write to:
  NASA STI Help Desk
  NASA Center for AeroSpace Information
  7121 Standard Drive
  Hanover, MD 21076-1320

Comparison of a 3-D CFD-DSMC Solution Methodology With a Wind Tunnel Experiment

Christopher E. Glass and Thomas J. Horvath
Langley Research Center, Hampton, Virginia

August 2002

Comparison of a 3-D CFD-DSMC Solution Methodology With a Wind Tunnel Experiment

Christopher E. Glass* and Thomas J. Horvath*

NASA Langley Research Center, M/S 408A, Hampton, VA, USA 23681-2199

Abstract.
   A solution method for problems that contain both continuum and rarefied flow regions is presented. The methodology is applied to flow about the Mars Sample Return Orbiter (MSRO), a 3-D blunt body, which contains a region of highly compressed forebody flow, a shear layer where the flow separates from a forebody lip (i.e., where the base plane intersects the forebody), and a low density wake region about the afterbody. Because the blunt body flow contains such disparate regions, employing a single numerical technique to solve the entire flow field for a 3-D configuration is often impractical, or the technique does not apply. Direct simulation Monte Carlo (DSMC) could be employed to solve the entire flow field; however, the technique would require inordinate computational resources for continuum to near continuum regions, since, it is best suited for the rarefied wake region. Computational fluid dynamics (CFD) is appropriate for the high-density region on the forebody, but in the rarefied wake region, continuum assumptions do not apply. This problem poses a situation where the CFD-DSMC approach presented herein may be a suitable way to obtain a higher fidelity solution.

INTRODUCTION

A mission to collect terrestrial material from Mars and return it to Earth for detailed analysis was under consideration. The approach for the sample return mission called for a joint US/European mission [1, 2, 3, 4]. Key elements of this mission profile are highlighted in Fig 1. Collected surface samples would be placed into Mars orbit in advance of the arrival of a second vehicle, a French designed [5] Mars sample return orbiter (MSRO). Upon planetary approach, the MSRO vehicle would perform an aerocapture maneuver in the Martian atmosphere with a blunt aeroshell. An Earth entry vehicle (EEV) and sample retrieval hardware on the MSRO would reside behind the aeroshell during the aerocapture maneuver. Proper positioning of this hardware is essential to avoid thermal damage from localized near
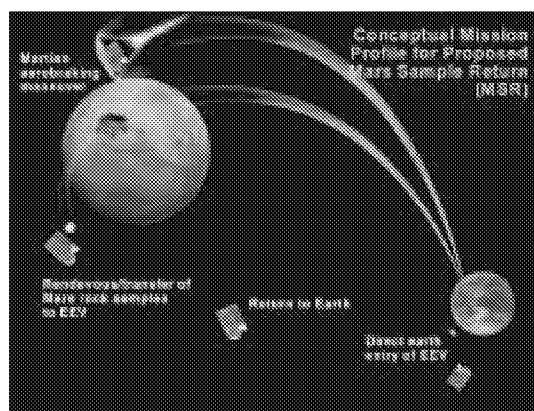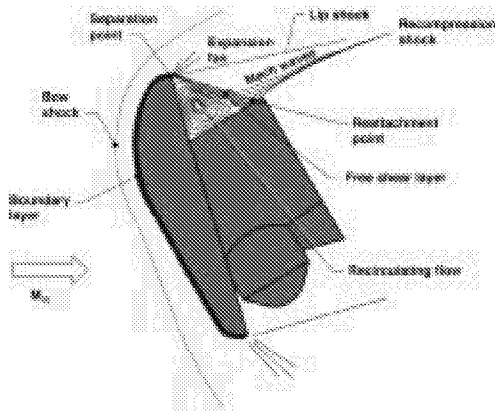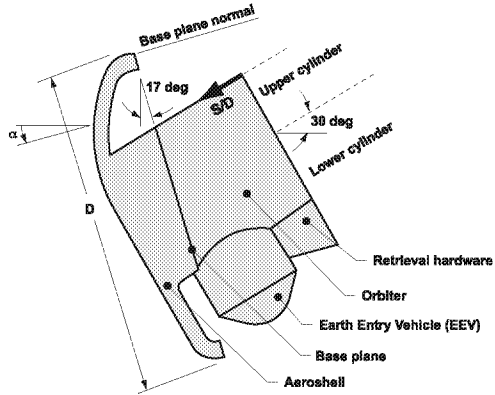

FIGURE 1.   Elements of proposed Mars sample return mission.

FIGURE 2. Sketch of blunt body wake flow field region from hypersonic environment.

FIGURE 3. Sketch of the proposed Mars sample return orbiter.

wake phenomenon. Although convective heating rates to payloads behind aerobrakes may be low [6], high localized heating can occur if, after separating from the aeroshell, the boundary layer impinges on the afterbody as a shear layer [7, 8, 9, 10]. This complex hypersonic blunt body base flow is shown schematically in Fig. 2.

The Outer Mold Lines (OML) of the proposed MSRO vehicle, shown in Fig. 3, represents a reference baseline for conducting experimental and computational wake assessments. The vehicle consists of a drag brake (aeroshell) and a base-mounted cylindrical afterbody. The aeroshell base is concave as shown in Fig. 3 and based on a design detailed by Cheatwood [11], originally proposed in support of the Aeroassist Flight Experiment (AFE). At 0 ° angle-of-attack, the free stream is aligned with the minor axis of the ellipsoidal nose. Also shown in the figure are the EEV and retrieval/transfer hardware on the afterbody.

DATA SOURCES

Experimental Study. The MSRO configuration was experimentally studied [12] in the NASA Langley Research Center 20-Inch Mach 6 CF_4 Tunnel [13]. Hypersonic measurements of afterbody heating were performed in tetraflouromethane (CF_4) test gas because it provides high density ratios across strong shock waves, which simulates hypersonic reacting gas flow conditions in flight. In addition, experimental data at the low-density condition of the facility [13] provides a validation opportunity of the CFD-DSMC technique.

For the experiment, the OML of the MSRO configuration were taken from a grid provided by Gnoffo [3]. Because the wind tunnel model was 2.8% scale (to avoid tunnel blockage), the model-scaled aeroshell thickness would be about 2mm. Concerns of casting and post-cast integrity resulted in thickening the model aeroshell lip about twice as thick as scale. The ceramic models were coated with thermographic phosphors that allow surface temperature mappings of the model. With temperature images acquired at different times in an experiment, global heating images are computed.

The purpose of the experiment was to study flow impingement on the afterbody, and if present, determine the location and magnitude of the heating peak for comparison with prediction. Prediction methods that accurately determine near wake characteristics of blunt bodies are desired to reduce conservative design margins for this class of planetary entry vehicles.

Numerical Technique. The purpose of this study is to present a CFD-DSMC numerical technique and compare its results with those from the wind tunnel experiment described previously. The specific details of the technique are given in the next section. However, generally, the same approach as previously reported [3] for the aerobraking MSRO is utilized: First, a solution for the entire flow field is obtained with CFD [14]. Then, the CFD solution is examined to identify regions of continuum flow and transitional and rarefied flow that require a solution technique such as DSMC. Next, a dataset is extracted from the CFD flow field along a plane that separates the two regimes, which, for this case, lies on the aeroshell lip. Note that the plane is chosen so that the flow upstream of the boundary is not influenced by

downstream conditions. Finally, DSMC is performed on the downstream region to obtain the wake flow field solution. The numerical techniques used in this study are GASPv4 [14] for the CFD and DAC [15] for the DSMC.

Because the wake region for this study is near-continuum, a technique is developed and employed that reduces the resource requirement to do the DSMC simulations. The technique requires that cells near the wall have cell Knudsen numbers (a measure of the local mean free path to the cell size), Kn_{cell}, near order one, but away from the wall the value may be considerably less, hence, allowing more molecular collisions near the wall where the flow field gradients are generally large and, thus, more critical for determining surface properties.

SOLUTION METHODOLOGY

In this section, the CFD prediction of the MSRO flow field is presented and analyzed to show the degree of wake rarefaction. After establishing the need for DSMC in the wake, a method is presented that provides a DSMC wake solution employing a boundary condition from the CFD flow field solution. An adaptive grid routine is presented that substantially reduces the DSMC resource requirements for wake simulations. In the next section, the flow field results from both the CFD and CFD-DSMC are compared, and surface heating from the experiment, CFD, and CFD-DSMC is discussed.

Computational Fluid Dynamics. CFD was performed using the GASPv4 code [14]. Thermodynamic properties of CF_4 were not included in the default database for GASP; therefore, the Lewis curve fits for the thermophysical properties, as compiled by McBride, et al. [16], and the transport properties, as documented by Sutton [17], formed the GASP compatible gas model.

Tests in the Langley wind tunnels are accompanied with a standard run sheet, which contains free stream test conditions and theoretical stagnation point heating on a sphere using methods similar to those developed by Fay and Riddell [18]. The reference radius for the present study is 45.97 mm, which approximates the ellipsoidal nose radius of the model-scale MSRO AFE forebody in the plane of symmetry. The sphere flow field and stagnation point heating values were computed using the CF_4 GASP compatible gas properties.

A two-block 380 thousand cell grid created without a singularity at the stagnation point was chosen for the sphere heating calculation. The calculation was performed with sequence meshing; that is, a solution was first obtained on a coarse grid, then a medium grid, and finally on the fine grid. T_{wall} = 300 K, with the free stream properties of the CF_4 tunnel test conditions of ρ_∞ = 0.001526 kg/m^3, T_∞ = 201.1 K, and V_∞ = 907.4 m/sec, which provides a γ_∞ = 1.21 stream of M_∞ = 6.0 flow.

The solution process consisted of using a 3rd-order, upwind-biased Roe and vanLeer flux-splitting scheme, with the Roe scheme imposed in a direction normal to the sphere surface. The flow was assumed steady and laminar throughout. The full Navier-Stokes equations (including both the thin-layer and cross-flow terms) were applied for the flow field calculation. Also, the equations were integrated globally using the Gauss-Seidel implicit time marching scheme. The sphere heating calculation resulted in a stagnation point value of q_{ref} = 21,300 W/m^2, which is used as a reference value to normalize heating data presented in this document. The calculated stagnation point heating was within 5% of the theoretical value of 22,400 W/m^2. Because of the close agreement, it was deemed that a valid gas model for CF_4 was employed for the CFD calculation.

Next, the flow field for the 2.8% model-scaled MSRO configuration was computed for the $\alpha = -4°$ condition to match the experiment. The grid consisted of 70 blocks with over 5 million cells to the symmetry plane. Generally, the same method employed for the sphere was used for the MSRO calculation. An exception was with the flux-splitting formulation: the Roe and vanLeer scheme utilized only the thin-layered terms of the Navier-Stokes equations for the forebody, and a Roe scheme with all terms was employed in the afterbody wake flow field. Similarly, the solution was grid sequenced. Because of the grid size, the solution was performed on 128 processors of an SGI Origin 2000 supercomputer.

Fig. 4 is a symmetry plane view of the fine grid MSRO flow field density contours. The orientation partially shows the flow in the scalloped backside of the aeroshell. A high-density shock wraps about the forebody, and a low-density wake develops along the backside. Aft of the aeroshell lip, the contours show a very low-density region.

Analysis of Wake Flow Field. Because the wake shown in Fig. 4 has regions of low-density flow, the Knudsen number, $Kn_L = \lambda/L$, was calculated from the symmetry plane CFD flow field as it provides a measure of flow rarefaction in the region. The local mean free path, λ, is normalized by the shell lip thickness of 2 mm. The shell
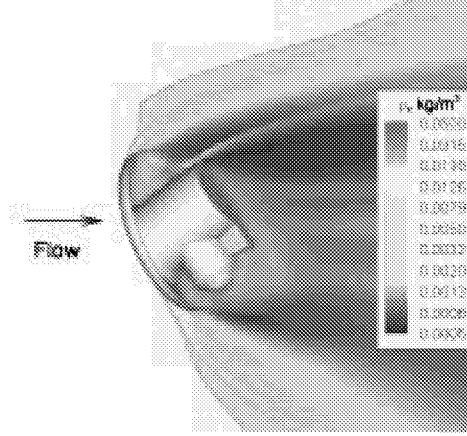
FIGURE 4. Density contour flow field about the MSRO calculated by CFD ($\rho_\infty = 0.00153$ kg/m^3).
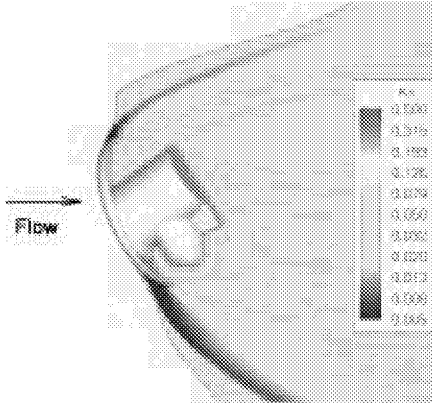
**FIGURE 5.** Knudsen number contours about the MSRO from the CFD flow field calculation.
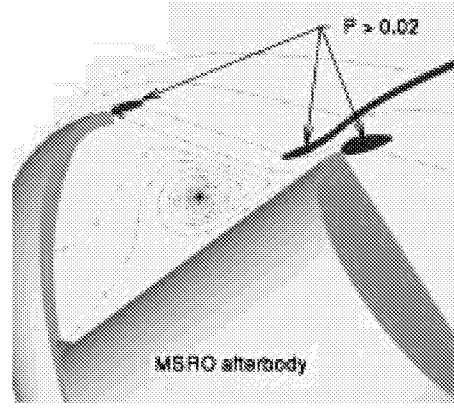
FIGURE 6. Rarefied regions in the MSRO wake identified by continuum breakdown parameter, P, greater than 0.02.

lip thickness was chosen as the critical dimension because the flow expands about the lip and thus greatly influences the wake flow near the shear layer, which impinges on the afterbody.

Shown in Fig. 5 are the Knudsen number contours in the wake region. Generally, for $0.01 \leq Kn_L \leq 10$, the flow is considered the transitional regime, and as Kn_L increases further the flow is rarefied. Fig. 5 shows that the majority of the symmetry plane wake is transitional; especially behind the afterbody (colored green to yellow) and the flow that expands around the lip of the aeroshell, which is colored green. Because the Kn_L uses an arbitrary length, in this case the aeroshell lip thickness, as a scaling constant for the entire flow field, a better measure of rarefaction for expanding flows is the continuum breakdown parameter, P. Like the Kn_L, P identifies regions of non-continuum flow; however, unlike Kn_L, the length scale for P is based on the local density and its gradient. It has been determined, for $P > 0.02$ [19], the flow is rarefied because the local flow gradients exceed those for which the continuum assumption is valid.

Fig. 6 shows the results of a calculation of the continuum breakdown parameter from the CFD solution. The figure presents a close view of the upper aeroshell lip and MSRO afterbody with regions where $P > 0.02$ on the symmetry plane. Also, stream traces are included on the figure to show the near body, wake region flow direction. Note that $P > 0.02$ as the flow expands about the aeroshell lip and the MSRO afterbody, as shown by the darkened gray regions on the figure. Because both Figs. 5 and 6 show these transitional regions, the wake region flow must be treated as non-continuum, and calculations of the wake should be performed, if practical, by a non-continuum method such as DSMC.
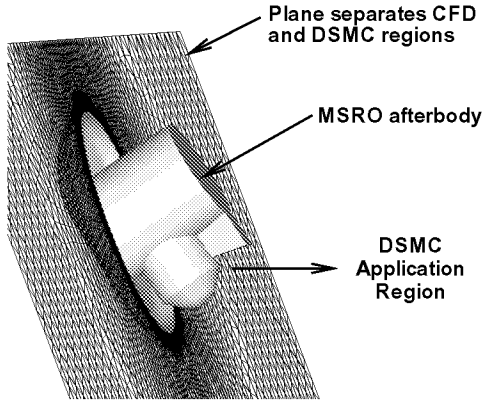
FIGURE 7. Plane separating CFD and DSMC solution regions.
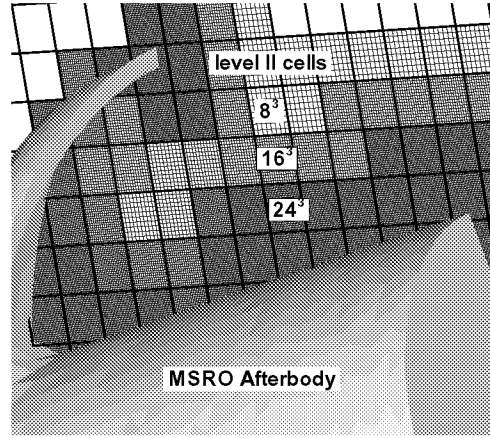
FIGURE 8. Symmetry plane DSMC grid showing gradient adaptation.

Direct Simulation Monte Carlo. DSMC results presented in this section were generated using the three-dimensional DAC code of LeBeau [15], which was previously employed for the MSRO Mars aerobraking conditions [3]. Specifics of the code, capabilities, description of geometric modeling, and boundary conditions are given in Ref. [15]. In general, DAC is a suite of DSMC pre-processing, processing, and post-processing codes, which use triangulated geometries that clip into a Cartesian grid of level I and adapted level II cells. The suite of codes with the MPI parallel-processing option was used in the current study. A significant feature of DAC is the ability to pre-process an adapted grid based on a previous DAC solution using user-controlled cell spacing. Additionally, because there was no CF_4 model for this study in the DAC database, the molecular properties for the DSMC gas file were obtained from properties presented by Sutton [17].

Shown in Fig. 7 is the triangulated plane (with 10,385 elements) that serves as the interface between the CFD and DSMC computations and the MSRO afterbody that defines a boundary for the DSMC wake region. The plane, which passes through the flow field at the MSRO aeroshell lip, was chosen to separate the continuum and non-continuum portions of the flow because it locates the expanding flow about the lip and afterbody wake flow in the DSMC domain. It is a natural division of the flow field between the forebody (on the left) and afterbody (on the right) where flow through the plane is in the downstream direction, thus no information is fed upstream from the DSMC. The plane is populated with the appropriate values of number density, velocity components, and temperature by interpolating and/or extrapolating them from the CFD solution. Also, the MSRO afterbody surface, which is shaded on gray and consists of 10,017 triangular elements, is shown on the figure.

The DSMC solution procedure employed by DAC first involves establishing a uniform grid of level I cells to produce an initial flow field. Next, grid adaptation is performed, which creates level II cells within the level I cells where more cell resolution is required. Ideally, the adaptation process continues until the grid fully resolves the flow field with cells sized to the order of a local mean free path.

With the current wake flow problem having pockets of rarefied flow, DSMC would appear to be the appropriate method for simulating the flow. However, a further analysis of the CFD wake region based on the local mean free path shows that to fully resolve the flow using DSMC, the number of cells for this problem would be inordinate (of the order 10^{11}). Therefore, a special cell adaptation method was developed to capture the near wall gradients with level II cells, but relax the cell requirement away from the wall (flow may not be fully resolved). Additionally, it was decided to limit the maximum number of molecules for the present case to between 150 to 200 million (20 million cells) because of computational demands (A 200 million molecule simulation requires memory of over 18 Gbytes of core to execute and about 12 Gbytes of disk space to write the working files.).

The present grid adaptation scheme employs a user specified gradient of level II cells from the surface. Specifically, the number of level II cells is maximized near the wall and decreases away from the wall. A characteristic distance, d_I, the level I cell diagonal, controls adaptation. At $4d_I$ and greater from the wall, no level II cell adaptation is allowed. For $3d_I$, the maximum number of level II cells is restricted to one-third of the wall value in each of the coordinate directions, and for $2d_I$, the maximum number in each direction is two-thirds of the of the wall value. The scheme is

5

TABLE 1. Results of level II cell adaptation on the maximum shear layer impingement heating.

Simulated Molecules [$x10^{-6}$]	q/q_{ref}*	location, s/D	Kn_{cell}	% difference from last adaptation
0.083	1.290	.025	.01	305.7
4.7	0.448	.073	.06	40.9
34.	0.376	.084	.07	18.2
65.	0.360	.076	.09	13.2
100.	0.346	.075	.11	8.8
150.	0.330	.074	.13	3.8
200.	0.318	.073	.15	—

* q_{ref} = 21,284 W/m^2

illustrated in Fig. 8, which shows a symmetry plane cut through the solution adapted DSMC grid. The level I cells are enclosed by the heavier, regularly spaced lines, and the level II cells are surrounded by the lighter, finer grid within the level I cells. For the case shown in Fig. 8, the maximum number of level II cells near the wall is restricted to 24 in each of the three orthogonal directions (finest grid of the study) and labeled 24^3. For $2d_I$, the cell is identified with 16^3 indicating that in each direction two-thirds of the maximum spacing is in effect. Likewise, for $3d_I$, the level II cell spacing is one-third of the maximum in any direction, with 8^3 cells. Although any number of schemes can be used, this one was employed because it seemed to give consistently good computational performance and it limited the number of simulated molecules for this case to about 200 million for the final adaptation.

To get to the 200 million molecule case, seven DSMC solutions of the MSRO wake flow field were performed. The first two were for the uniform grid and an adaptation. The following cases employed the gradient adaptation methodology described above for 12, 15, 18, 21, and 24 maximum number of cells in each direction. Close attention was paid to the shear layer surface heating on the cylinder, its location, the cell Knudsen number (Kn_{cell}) at the location of shear layer impingement and the percent difference in heating between the subsequent DSMC solutions. Results from these solutions are given in Table 1.

Table 1 provides an accounting of the similarities and differences in the MSRO wake DSMC solution as the grid is refined using the gradient adaptation method. Specifically, from 34 to 200 million molecules, heating changed only 18%, and the impingement point moved from s/D = .084 to .073. For the larger molecule simulation comparisons, the change in heating and impingement point location was less: With heating, 9% for the 100 million molecule case and 4% for the 150 million molecule case using the 200 million molecule case as a baseline, and for the impingement point location, Δs/D = .001 between each case.

Although the change in location and heating difference from shear layer impingement did not go to zero, they did decrease. Because of the size limitations imposed on the problem (200 million molecules), the solution adaptation was stopped. As will be seen in the next comparisons, even though a completely resolved DSMC flow field was not attempted, the methodology developed provides useful information for a near-continuum, transitional wake calculation using DSMC.

RESULTS

Flow Field Comparison. In this section, a flow field comparison between the two numerical schemes, that is, the CFD and the CFD-DSMC techniques, is presented for the symmetry plane shown in Fig. 9. CFD is performed about the entire configuration, and the DSMC flow field solution begins along the plane shown on Fig. 7, which is at the forebody lip. Note that the MSRO configuration has a backside cavity that allows fluid to collect and that supports a wake closure shear layer. The same scaled-size cavity region was used for both the CFD and CFD-DSMC solutions.

As shown by the stream traces on Fig. 9, the free stream flow direction is from left to right. Density contours of the flow field are also presented. A comparison of the density contours about the afterbody shows that the CFD solution produces a higher density wake flow field than the CFD-DSMC solution. This observation is consistent with previous studies [20] of blunt body wakes. Stream traces for CFD ride over and graze the rear of the afterbody cylinder where the high density region is located (See the yellow shaded region.). For the CFD-DSMC solution, the stream traces show direct impingement of the shear layer on the afterbody cylinder (See Fig. 9(b).); however, the density increase
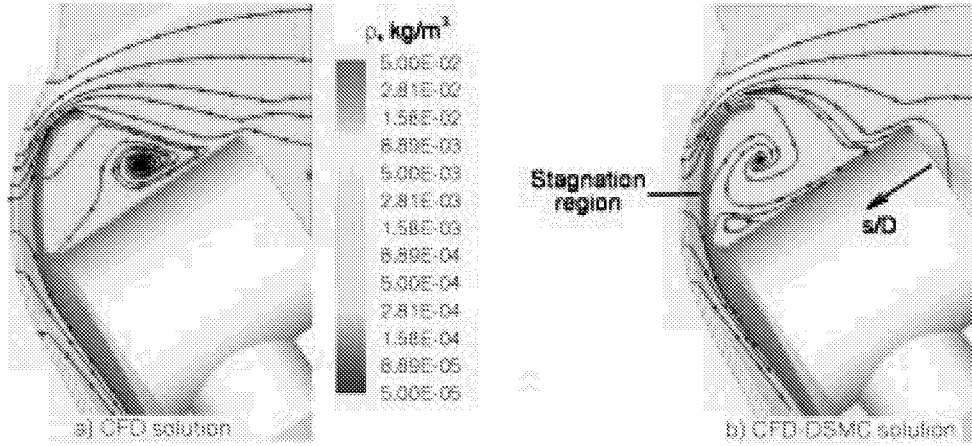
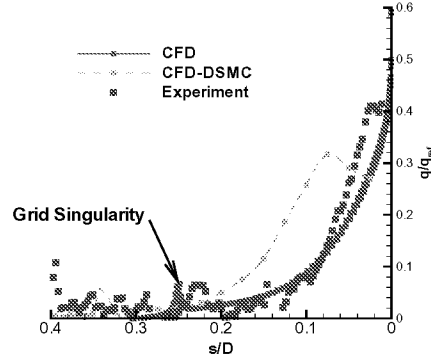**FIGURE 9.** Flow field surrounding MSRO from CFD and CFD-DSMC.

FIGURE 10. Heating comparison between CFD, CFD-DSMC, and experiment.

at the shear layer impingement is not as high as the density increase at the grazing shear layer location predicted by CFD. Also, the stream traces for the CFD-DSMC solution show a secondary vorticity near the forward end of the shell cavity, but CFD does not.

Afterbody Surface Heating Comparison. A comparison of normalized surface heating between the CFD, CFD-DSMC, and the wind tunnel experiment is presented in Fig. 10. The configuration for all three cases is the same, except, as noted earlier, the aeroshell thickness of the wind tunnel model is about twice that of the numerical models (4 mm vs. 2mm, respectively) because of casting and model integrity concerns.

The maximum heating predicted by CFD is greater than both the experiment and the CFD-DSMC values. The CFD shear layer grazes the aft portion of the cylinder and results in the CFD heating distribution increasing to a value of $q/q_{ref} = 0.6$ without a peak before s/D goes to zero. The maximum CFD heating at $s/D = 0$ is 46% higher than the maximum experiment value ($q/q_{ref} = 0.41$ at $s/D = 0.022$). In addition, the CFD heating decreases monotonically with increasing s/D, except at the CFD grid singularity ($s/D = 0.25$) where a small peak is observed.

The comparison shown in Fig. 10 between the CFD-DSMC solution and the experiment is an improvement over the CFD solution. The CFD-DSMC solution shows that the shear layer impinges the surface at $s/D = 0.075$ with a normalized heating rate value of 0.32. Also, shear layer impingement is evidenced in Fig. 9(b) where the stream trace impacts the wall. When compared to the peak experimental value, the CFD-DSMC solution is 22% lower. In addition, the CFD-DSMC distribution provides some of the same off-peak features as the experimental results, such as the undulations in each for $s/D > 0.2$. Although the CFD-DSMC results qualitatively agree with the experiment,

7

there are differences in the heating levels and impingement location. The experimental uncertainly in surface heating is quoted as $\pm 15\%$ [12], which may account for the heating difference, but not the difference in impingement location. Differences may be attributed to the thicker experimental aeroshell that would allow the shear layer to be positioned further outboard and cause the shear layer to impinge closer to the cylinder end.

CONCLUDING REMARKS

A numerical study was performed for a 2.8% model of a proposed Mars Sample Return Orbiter (MSRO). A shear layer is formed from the aeroshell boundary layer spilling off the forebody and impinges on the afterbody. Conditions of a low-density, Mach 6, CF_4 experiment of the MSRO model with a wake shear-layer impingement were chosen to demonstrate details of a 3-D CFD-DSMC technique, which has been developed and is discussed. Because the region of interest in the wake is in the transitional regime and would require an inordinately sized DSMC problem, a near-wall cell gradient adaption scheme was developed and is demonstrated. A comparison between the 3-D CFD-DSMC solution and the experiment showed they were qualitatively similar and differences may be attributed to experimental uncertainty and model aeroshell non-conformity. The demonstrated CFD-DSMC technique with cell gradient adaptation shows much promise for performing DSMC in the transitional regime where traditional application of DSMC is not possible, and CFD alone does not produce credible results.

REFERENCES

1. Mitcheltree, R. A., Kellas, S., Dorsey, J. T., Desai, P. N., and Martin, C., A passive Earth-entry capsule for Mars sample return, Tech. Rep. AIAA Paper 98-2851 (1998).
2. Amundsen, R. M., Dec, J. A., Mitcheltree, R. A., Lindell, M. C., and Dillman, R. A., Preliminary thermal analysis of a Mars sample return earth entry vehicle, Tech. Rep. AIAA-2000-2584 (2000).
3. Glass, C., and Gnoffo, P., "A 3-D Coupled CFD-DSMC Solution Method with Application to the Mars Sample Return Orbiter," in *Proceedings of the 22nd International Symposium of Rarefied Gas Dynamics*, 2000, presented as paper 4003, also available as NASA/TM-2000-210322.
4. Gnoffo, P. A., Computational aerothermodynamics in aeroasist applications, Tech. Rep. AIAA Paper 2001-2632 (2001).
5. Chanetz, B., *Study of the Mars Sample Return Orbiter in the Hypersonic Wind Tunnel R5Ch*, Arcachon, France, 2001.
6. Gnoffo, P. A., Planetary-entry gas dynamics, *Annual Review of Fluid Mechanics* (1999).
7. Horvath, T. J., McGinley, C. B., and Hannemann, K., Blunt body near wake flow field at Mach 6, Tech. Rep. AIAA Paper 96-1935 (1996).
8. Horvath, T. J., and Hannemann, K., Blunt body near wake flow field at Mach 10, Tech. Rep. AIAA Paper 97-0986 (1997).
9. Hollis, B. R., Experimental and computational aerothermodynamics of a Mars entry vehicle, Tech. Rep. NASA CR 201633 (1996).
10. Wells, W. L., Measured and predicted aerodynamic heating on a cylinder in wake of afe configuration at incidence, Tech. Rep. AIAA Paper 89-2162 (1989).
11. Cheatwood, F. M., DeJarnette, F. R., and Hamilton, H. H. I., Geometrical description for a proposed aeroassist flight experiment vehicle, Tech. Rep. NASA TM-87714 (1986).
12. Horvath, T., Heiner, N., Olguin, D., Cheatwood, F., and Gnoffo, P., Afterbody heating characteristics of a proposed Mars sample return orbiter, Tech. Rep. AIAA-2001-3068 (2001), presented at the 35th AIAA Thermophysics Conference, 11-14 June 2001, Anaheim, CA.
13. Miller, C., Langley hypersonic aerodynamic/aerothermodynamic testing capabilities-present and future, Tech. Rep. AIAA-1990-1376 (1990).
14. AeroSoft, *GASP Version 4 Reference Guide*, AeroSoft, Inc., Blacksburg, VA, 2001, website: http://www.aerosft.com/.
15. LeBeau, G., A Parallel Implementation of the Direct Simulation Monte Carlo Method, *Comput. Methods Appl. Mech. Engrg.*, **174**, 319–337 (1999).
16. McBride, B. J., Stanford, G., and Reno, M. A., Coefficients for Calculating Thermodynamic and Transport Properties of Individual Species, Tech. Rep. NASA Technical Memorandum 4513, NASA (1993).
17. Sutton, K., Relationships for the Thermodynamic and Transport Properties in the testing Environment of the Langley Hypersonic CF_4 Tunnel, Tech. Rep. NASA Technical Memorandum 83220, NASA (1981).
18. Fay, J. A., and Riddell, F. R., Theory of stagnation point heat transfer in dissociated air, *Journal of Spacecraft and Rockets*, **25** (1958).
19. Bird, G., *Molecular Gas Dynamics and the Direct Simulation of Gas Flows*, Clarendon Press, 1994, ISBN 0-19-856195-4.
20. Moss, J., Mitcheltree, R., Dogra, V., and Wilmoth, R., Direct Simulaation Monte Carlo ans Navier-Stokes Simulations of Blunt Body Wake Flows, *AIAA Journal*, **32**, 1399–1406 (1994).

REPORT DOCUMENTATION PAGE

1. REPORT DATE *(DD-MM-YYYY)* 08-2002	2. REPORT TYPE Technical Memorandum	3. DATES COVERED *(From - To)*

4. TITLE AND SUBTITLE
Comparison of a 3-D CFD-DSMC Solution Methodology With a Wind Tunnel Experiment

5a. CONTRACT NUMBER

5b. GRANT NUMBER

5c. PROGRAM ELEMENT NUMBER

6. AUTHOR(S)
Glass, Christopher E.; and Horvath, Thomas J.

5d. PROJECT NUMBER

5e. TASK NUMBER

5f. WORK UNIT NUMBER
706-85-42-01

7. PERFORMING ORGANIZATION NAME(S) AND ADDRESS(ES)
NASA Langley Research Center
Hampton, VA 23681-2199

8. PERFORMING ORGANIZATION REPORT NUMBER
L–18212

9. SPONSORING/MONITORING AGENCY NAME(S) AND ADDRESS(ES)
National Aeronautics and Space Administration
Washington, DC 20546-0001

10. SPONSOR/MONITOR'S ACRONYM(S)
NASA

11. SPONSOR/MONITOR'S REPORT NUMBER(S)
NASA/TM–2002–211777

12. DISTRIBUTION/AVAILABILITY STATEMENT
Unclassified-Unlimited
Subject Category 34
Availability: NASA CASI (301) 621-0390   Distribution: Standard

13. SUPPLEMENTARY NOTES

14. ABSTRACT
A solution method for problems that contain both continuum and rarefied flow regions is presented. The methodology is applied to flow about the 3-D Mars Sample Return Orbiter (MSRO) that has a highly compressed forebody flow, a shear layer where the flow separates from a forebody lip, and a low density wake. Because blunt body flow fields contain such disparate regions, employing a single numerical technique to solve the entire 3-D flow field is often impractical, or the technique does not apply. Direct simulation Monte Carlo (DSMC) could be employed to solve the entire flow field; however, the technique requires inordinate computational resources for continuum and near-continuum regions, and is best suited for the wake region. Computational fluid dynamics (CFD) will solve the high-density forebody flow, but continuum assumptions do not apply in the rarefied wake region. The CFD-DSMC approach presented herein may be a suitable way to obtain a higher fidelity solution.

15. SUBJECT TERMS
CFD, DSMC, transitional flow solution, MSRO

16. SECURITY CLASSIFICATION OF:

a. REPORT	b. ABSTRACT	c. THIS PAGE
U	U	U

17. LIMITATION OF ABSTRACT
UU

18. NUMBER OF PAGES
13

19a. NAME OF RESPONSIBLE PERSON
STI Help Desk (email: help@sti.nasa.gov)

19b. TELEPHONE NUMBER *(Include area code)*
(301) 621-0390